



GEWEX Cloud System Study (GCSS) cirrus cloud working group: modelling case development based on 9 March 2000 ARM SGP observations

H. Yang^{1,2}, S. Dobbie², G. G. Mace³, A. Ross², and M. Quante⁴

¹CMA Key Laboratory for Atmospheric Physics and Environment, Nanjing University of Information Science and Technology, no. 219 Ningliu Road, Nanjing, 210044, China

²School of Earth and Environment, Institute for Climate and Atmospheric Science, University of Leeds, Leeds LS2 9JT, UK

³Meteorology Department, University of Utah, 135 S 1460 East Rm 819 (WBB), Salt Lake City, UT 84112-0110, USA

⁴Helmholtz-Zentrum Geesthacht, Institute of Coastal Research/System Analysis and Modelling, Max-Planck-Straße 1, 21502 Geesthacht, Germany

Received: 16 September 2011 – Accepted: 14 October 2011 – Published: 24 October 2011

Correspondence to: H. Yang (huiyi.yang@physics.ox.ac.uk)

Published by Copernicus Publications on behalf of the European Geosciences Union.

Title Page

Abstract

Introduction

Conclusions

References

Tables

Figures

◀

▶

◀

▶

Back

Close

Full Screen / Esc

Printer-friendly Version

Interactive Discussion



Abstract

The GCSS working group on cirrus focuses on inter-comparison of model simulations for models ranging from very detailed microphysical and dynamical models through to general circulation models (GCMs). In the previous GCSS inter-comparison, it was a surprise to the modeling community how much of a range there was in ice water path predictions by different cirrus models for such idealized cases. There was some grouping according to the complexity of models; however, there were no observations with which to distinguish between model performance. The aim of the current GCSS cirrus inter-comparison is to base the study on a rigorously observed case study. In this way, the case may be used to identify which models in the inter-comparison are performing well and highlight areas for model development as well as provide a base case for future models to compare against when being developed or when testing new developments within existing models. In this paper, we present the case development for the current GCSS working group study on cirrus cloud. This paper summarizes how the case was developed and based on the 9 March 2000 Atmospheric Radiation Measurement (ARM) Southern Great Plains (SGP) intensive observation period (IOP). To our knowledge, this case offers the most detailed case study for cirrus comparison available, with extensive effort to derive the most appropriate large scale forcing as possible which is such a significant determinant of clouds. We anticipate this will offer significant improvement over past comparisons which have mostly been loosely based on observations. Notably this study makes use of retrievals of observations of ice water content, ice number concentration, and fall velocity, thus offering several constraints to evaluate model performance. The case study is developed utilizing various observations including ARM SGP remote sensing including the Millimeter cloud radar (MMCR), radiometers, radiosondes, aircraft observations, satellite observations, objective analysis and complemented with results from the Rapid Update Cycle (RUC) model output and bespoke gravity wave simulations using the 3-dimensional velocities over mountains (3DVOM) model. An initial modelling assessment of the case has been shown

GCSS WG2 – case study

H. Yang et al.

[Title Page](#)

[Abstract](#)

[Introduction](#)

[Conclusions](#)

[References](#)

[Tables](#)

[Figures](#)

[◀](#)

[▶](#)

[◀](#)

[▶](#)

[Back](#)

[Close](#)

[Full Screen / Esc](#)

[Printer-friendly Version](#)

[Interactive Discussion](#)



using the UK Met Office Large Eddy Simulation Model (LEM) which supports the use of this case for the full inter-comparison study.

1 Introduction

The Global Energy and Water Cycle Experiment (GEWEX) Cloud System Study Program (GCSS) was initiated by K. Browning and others in 1990. The purpose of GCSS is to develop better parameterizations of cloud systems within climate and numerical weather prediction models Randall et al. (2000). There were five initial Working Groups focusing on different clouds: boundary-layer clouds, cirrus clouds, extra-tropical layer cloud systems, precipitating deep convective cloud systems and polar clouds. This has been more recently extended to include other case developments such as Pacific Cross-section Intercomparison, etc. The cirrus working group (WG2) in the past has initiated one previous project focusing on high resolution cloud model inter-comparison. It was denoted the Idealized Cirrus Model Comparison Project (ICMCP) and had 16 models involved in the comparison ranging from Cloud Scale models (CSMs) to Single Column Models (SCMs) (both GCM SCMs as well as highly detailed 1-D models).

The results of the first inter-comparison (ICMCP) were a surprise to the cirrus community. It showed that the community's numerical models of cirrus showed significantly larger disagreement than expected concerning such fundamental quantities as ice water path (IWP) for even idealized cases. The results appeared only in a conference paper Starr et al. (2000). Figure 1 is taken from that paper and illustrates the range in results of as much as two orders of magnitude in IWP. There was some grouping noted between bin and bulk models; however, the range was large for all categories. The results from SCMs span the whole range of CSM results and heritage models exhibit larger scatter and generally there was larger scatter for all model categories for the cold case.

In addition to the ICMCP inter-comparison, there was also a Cirrus Parcel Model Comparison Project (CPMCP) (Lin et al., 2002) which was a follow-on project as part

GCSS WG2 – case study

H. Yang et al.

Title Page

Abstract

Introduction

Conclusions

References

Tables

Figures

◀

▶

◀

▶

Back

Close

Full Screen / Esc

Printer-friendly Version

Interactive Discussion



of the GCSS WG2. The main aim of their study was to compare the microphysics specification of different cirrus models under idealised conditions. For complete details, the reader is referred to Lin et al. (2002).

Although well instrumented sites such as ARM provide significant amounts of data for modeling studies, developing a high resolution modeling case based in observations is somewhat rare in the literature. Several studies have based their modeling studies on observations such as Brown and Heymsfield (2001) used TOGA-COARE data, Benedetti and Stephens (2001) used ARM data, Cheng et al. (2001) used FIREII data, Marsham and Dobbie (2005) and Marsham et al. (2006) used Chilbolton data, Solch and Karcher (2011) used ARM data, and Yang et al. (2011) used EMERALD1 data; however, these studies are only loosely based on observations and often the large scale forcing of the cloud layer, which is so important for cloud development (see Lin et al. 2002) is either not available or very approximate.

Comparisons to observations have improved in recent years in that efforts have been made to simulate the remote sensing of radar and radiometers within the models for ease of comparison when evaluating timeseries (Marsham and Dobbie, 2005; Marsham et al., 2006), as well as making use of more and more observations such as modelling returns of Doppler fall velocities Marsham et al. (2006). Important advances have been made by observationalists since the last inter-comparison in using a synergy of more than one instrument to improve retrievals (Deng and Mace, 2006; Delanoë and Hogan, 2008). Doppler radar as well as radiometers and radiosondes are used to determine ice content, ice number, and fall velocities. This offers great opportunities to test models since models can be easily tuned to a single observation of say ice water content (IWC) or ice number concentration (INC); however, observations of three or more variables affords a much better opportunity to highlight models performing well and also highlight potential deficiencies in models. We note that one case study is not a definitive assessment of the cirrus models but offers a good basis to begin with and build upon.

GCSS WG2 – case study

H. Yang et al.

[Title Page](#)

[Abstract](#)

[Introduction](#)

[Conclusions](#)

[References](#)

[Tables](#)

[Figures](#)

[⏪](#)

[⏩](#)

[◀](#)

[▶](#)

[Back](#)

[Close](#)

[Full Screen / Esc](#)

[Printer-friendly Version](#)

[Interactive Discussion](#)



GCSS WG2 – case study

H. Yang et al.

[Title Page](#)[Abstract](#)[Introduction](#)[Conclusions](#)[References](#)[Tables](#)[Figures](#)[◀](#)[▶](#)[◀](#)[▶](#)[Back](#)[Close](#)[Full Screen / Esc](#)[Printer-friendly Version](#)[Interactive Discussion](#)

It is important for the cirrus research community to assess current cirrus models and schemes against rigorous observations to determine if cirrus modelling has improved from the developments over the last decade and also use the results to gauge which models are performing well and identify areas for improvement. This is the first cirrus study that includes as rigorous as possible comparisons to observations with the added benefit of an inter-comparison framework. In this first paper, we describe the development of the modelled case based on the 9 March 2000 observations at the ARM SGP site. Included in this is a description of the observed case, what observations were available, what observations were required to establish the modelling study, and how the modelled case was established. This case was then issued to GCSS cirrus working group members to participate in the modelling inter-comparison; the results of which will be presented in a follow-on paper.

2 UK LEM model

To establish the modelling case based on the 9 March ARM SGP observations, we used the UK Met Office Large Eddy Model (LEM) v2.3 (Mace, 1998; Gray et al., 2001). The UK Met Office LEM performs numerical integrations using basic equations for momentum, thermodynamics, and continuity. The model is non-hydrostatic and uses the deep anelastic approximation (quasi-Boussinesq) which allows for small pressure and density variations from the reference hydrostatic state. Periodic boundary conditions are used at the horizontal edges of the domain and rigid lid conditions are used at the surface and top of model boundaries. The model has been used for several studies of cirrus (Dobbie and Jonas, 2001; Marsham and Dobbie, 2005; Marsham et al., 2006; Yang et al., 2011).

The version we use has a fully integrated Fu-Liou radiation scheme to address the radiative properties and heating rates of the cloud. Details of the radiation scheme are provided below and in papers such as Dobbie and Jonas (2001), Marsham and Dobbie (2005), and Marsham et al. (2006). We provide a brief description here. The radiation

GCSS WG2 – case study

 H. Yang et al.

[Title Page](#)
[Abstract](#)
[Introduction](#)
[Conclusions](#)
[References](#)
[Tables](#)
[Figures](#)
[I◀](#)
[▶I](#)
[◀](#)
[▶](#)
[Back](#)
[Close](#)
[Full Screen / Esc](#)
[Printer-friendly Version](#)
[Interactive Discussion](#)


model used is based on Fu and Liou (1992, 1993) with an ice radiation package Fu (1996); Fu et al. (1998) and is coupled with the LEM and used to assess cirrus radiative properties, as was done by Dobbie and Dobbie and Jonas (2001), Marsham and Dobbie (2005), Marsham et al. (2006), and Yang et al. (2011). The radiative transfer equation solution is derived using the discrete ordinates delta four-stream solution approach as discussed in Liou (1986) or papers such as Li and Dobbie (1997).

The Fu-Liou δ -four-stream model is a 1-D algorithm that is applied to all columns independently. The Fu-Liou radiation model has six solar and twelve infrared bands. The scheme is linked to the water in the LEM including ice, liquid droplets, rain, graupel, snow, and water vapour. For the case study, the optical properties are specified use the cloud ice water content and a value of generalised effective size of 35 μm (a similar approach also used in water clouds, see Dobbie and Jonas, 2001), which is in keeping with the observations after converting between generalised effective size and effective size and observations more generally (see Fu, 1996). Rayleigh scattering is treated for molecules and gaseous absorption is implemented using a correlated k-distribution method including gaseous absorption by O_3 , CO_2 , CH_4 , N_2O and H_2O . The CO_2 , CH_4 and N_2O are assumed to have uniform mixing ratios throughout the atmosphere with concentrations of 330, 1.6 and 0.28 ppmv, respectively.

3 9 March 2000 observations used in the case development

The main aim of the current GCSS cirrus inter-comparison was to compare the model results to observations to evaluate model performance. As mentioned, the last inter-comparison showed strong model-to-model variation for results such as ice water path with time for even such an idealised case. It is imperative that the cirrus community evaluate their models with observations in as rigorous a way as possible and through multiple comparisons. This case presented in this work forms the first step in that process.

GCSS WG2 – case study

H. Yang et al.

[Title Page](#)[Abstract](#)[Introduction](#)[Conclusions](#)[References](#)[Tables](#)[Figures](#)[I◀](#)[▶I](#)[◀](#)[▶](#)[Back](#)[Close](#)[Full Screen / Esc](#)[Printer-friendly Version](#)[Interactive Discussion](#)

The 9 March 2000 case was selected because it was a well observed case. During the intensive observing period (IOP) at the SGP ARM site in March 2000, cirrus formed just upwind from the site on the 9th and advected directly over the Central Facility (CF) site. The ARM sites have the most extensive set of routine measurement in the world and this is enhanced with aircraft and supplemental measurements during IOP periods. In addition to the extensive observations taking place, analysis of some key results from the 9th were readily available for the inter-comparison. This included remote sensing retrieval of cloud properties, analysis of aircraft observations, and objective analysis (Zhang et al., 2000).

3.1 Meteorology and profiles

The region of cirrus that eventually was observed at the CF was first noted as a jet stream maximum in a southwesterly flow that passed over the mountain ranges of central New Mexico. The cirrus thickened as the disturbance approached central Oklahoma and the cloud features appeared to organize into longitudinal bands. Satellite imagery suggested active development of individual features within these bands as the system passed over the CF. The character of the cirrus in the satellite plots as well as the large scale atmospheric flow suggests that the cloud may be forced by gravity waves from the neighboring mountains. The objective analysis predicted a weak lifting, whereas the Rapid Update Cycle (RUC) model indicated little to no ascent. This is explored further in the large scale forcing section below.

The radiosondes were released simultaneously at five locations at three hour intervals during 9 March including at the CF site and four sites surrounding the CF. These were used to construct the profiles, such as temperature, pressure, horizontal wind profiles, used in the case. The profiles indicated a temperature inversion near cloud top and a water vapour peak at 8–9 km, where the cloud is observed, as shown in Fig. 2.

3.2 Remote sensing

Visible satellite images were analysed from both GOES 8 and 10 for the time period from 00:30 to 23:30 UTC on 9 March 2000. In Fig. 3, the blue indicator (with the time of 14:00 UTC inside) points to the ARM SGP Central Facility site and the white arrow indicates the location where the cirrus cloud system was first observed to form upwind and south west of the CF. The cloud system is observed to brighten and become more extensive in subsequent visible imagery as it advects from the location of formation to the ARM SGP site. The cloud is observed by the Millimeter Cloud radar (MMCR) at the CF approximately 210 min after the time of formation, at 17:30 UTC.

The remote sensing of the cirrus cloud properties such as ice water content, ice number concentration, and ice particle fall speeds is crucial to the case study. An important reason for choosing this case study was that these cloud properties were already analysed (by G. G. Mace, Utah) and made available for this study (Mace, 1998). The retrieval is based on algorithms of using radar reflectivity and downwelling infrared radiances to evaluate the cirrus cloud microphysical properties (Matrosov et al., 1992; Matrosov et al., 1994). The layer-averaged properties of optically thin cirrus is applied, which is calculated by using the observational platforms at the ARM sites. The layer-mean particle size distribution (PSD) (Mace, 1998) is the main assumption in this method, in which a modified gamma function (Dowling and Radke, 1990) is used. The PSD equation is

$$N(D) = N_x \exp(\alpha) \left(\frac{D}{D_x} \right) \exp \left(-\frac{D}{D_x} \right) \quad (1)$$

where D_x is the modal diameter, N_x is the number of particles per unit volume per unit length at the functional maximum, and α is the order of the distribution, which is suggested ≤ 2 for cirrus (Dowling and Radke, 1990).

Shown in Fig. 4 is the retrieved ice water content, ice number concentration, effective size, and mean mass length, etc as functions of time. The inter-comparison focuses

Title Page

Abstract

Introduction

Conclusions

References

Tables

Figures

◀

▶

◀

▶

Back

Close

Full Screen / Esc

Printer-friendly Version

Interactive Discussion



on when the cirrus first arrives at the SGP CF site which is the left-most portion of the retrievals in Fig. 4. It is evident in the retrievals that the cloud increases in ice water content as it advects over the SGP site and thickens in the vertical.

3.3 Aircraft turbulence observations

5 University of North Dakotas Cessna Citation aircraft undertook 12 flights as part of the IOP, in the March 2000, including flight penetrations at different altitudes through the cirrus cloud on the 9th. This flight started at 18:32 h which is after the first cloud had appeared at the CF, so it is not an exact match with our comparison time. But it appears reasonable to assume that the turbulence observed by the aircraft measurements is representative for the cloud at an earlier stage. The mean wind and wind turbulence were measured by five-hole-probe (Validyne P40d) in combination with INS/GPS (Litton LTN-76). The sampling rate is 25 Hz and the uncertainty for turbulent fluctuations is about 0.05 m s^{-1} . The true airspeed to estimate length scales was mostly about 120 m s^{-1} . The power spectra of the vertical wind velocity, w , along flight legs at different altitudes, as shown in Fig. 5, indicates a scale separation at about 320 m length scale (roughly 0.4 Hz). The scale of large eddies is about 200 meters (roughly 0.6 Hz) and the inertial sub-range starts showing up at a scale of about 100 m (roughly 1.2 Hz). The power spectra indicates that the turbulent kinetic energy is considerably higher in the cloud top region compared to the base. Based on the scale lengths deduced from the turbulence observations, we decided that 100 m grid resolution in the cloud layer for the LEM simulations would be appropriate.

3.4 Large scale forcing

The large scale forcing is critical in obtaining a good modelling case study, as it has such as important influence on the formation and magnitude of the cloud. For the March 2000 IOP at the ARM SGP site, objective analysis has been performed to assess the large scale forcing so we begin with this for our case.

Title Page

Abstract

Introduction

Conclusions

References

Tables

Figures

◀

▶

◀

▶

Back

Close

Full Screen / Esc

Printer-friendly Version

Interactive Discussion



3.4.1 Objective analysis

Objective analysis has been performed for the March 2000 IOP and results are summarised in Zhang et al. (2000). We summarise key points from the paper below; for specific details of the method please refer to Zhang et al. (2000). The objective analysis used is a variational analysis method (CVAM) which was originally developed by Zhang and Lin (1997) with a second improvement in 2000. CVAM was developed for deriving large-scale vertical velocity and advective tendencies from sounding measurements and works with the raw data from even a small number of stations. It can refine these atmospheric state variables as well as give uncertainties in the original data. The CVAM approach requires large-scale variables (u, v, T, q), surface measurements including surface sensible and latent heat fluxes, precip, surface pressure, surface winds, surface temperature, surface broadband net radiative flux, and column total cloud water.

The observed data for these variables are used in this analysis which includes conservation of column-integrated mass, water, energy, and momentum (Zhang et al., 2000). The data used in the CVAM approach are variables collected from the ARM balloon-borne sounding and National Oceanic and Atmospheric Administration (NOAA) wind profile measurements. Figure 6a shows there is one balloon launch site located at the CF of the ARM site and another four launch sites around the CF at the boundary facilities.

During the IOP 2000, sounding balloons were launched every three hours to measure the variables such as temperature, pressure, water vapour mixing ratio and wind profiles. In addition, the objective analysis makes use of seventeen NOAA wind profilers surrounding the SGP site. Seven of which are near the CF and five vertical profilers exactly overlap with the sounding stations, as shown in Fig. 6b. The seven sites constitute the domain of the objective analysis. One additional grid point is added in each boundary site to improve the linear assumption (Fig. 6c). The Cressman scheme (Cressman, 1959) is used for the upper air measurement, making use the general

GMDD

4, 2751–2790, 2011

GCSS WG2 – case study

H. Yang et al.

Title Page

Abstract

Introduction

Conclusions

References

Tables

Figures

◀

▶

◀

▶

Back

Close

Full Screen / Esc

Printer-friendly Version

Interactive Discussion



weighting function according to:

$$w_{ik} = w(x_i, x_k) = \begin{cases} \frac{1}{N} \frac{L^2 - (x_i - x_k)^2}{L^2 + (x_i - x_k)^2}, & d_{ik} < L \\ 0, & \text{otherwise} \end{cases} \quad (2)$$

where the w_{ik} is the weighting coefficient, k indicates the observational points and i is the analysis grid point, x_i is any variable in three or four dimensions at the grid point, x_k ($k = 1, 2, \dots, K$), observation stations, N_i is the number of measurements within distance L , and d_{ik} is the distance between the measurements and grid point.

The output from NOAA Rapid Update Cycle (RUC) is used in Eq. (3) as the value for the background function, f_b (shown in Fig. 6d). The general form used to evaluate the objective analysis variables at each grid-point is given by:

$$f_a(x_i) = f_b(x_i) + \sum_{k=1}^{k=K} w_{ik} [f_o(x_k) - f_b(x_k)] \quad (3)$$

For further details refer to Zhang et al. (2000). There is also a comprehensive set of surface measurements, as indicated in Table 1, around the SGP site and measurements from satellites such as GOES.

There are three frequently used area-based data analysis approaches for objective analysis including the analytical fitting method, the line integral method and the regular grid method. The ARM SGP objective analysis method uses a hybrid approach of the regular-grid and line integral methods and a variational constraining procedure (Zhang and Lin, 1997). The large scale variables diagnosed from the objective analysis are listed in Table 2.

From the objective analysis, we illustrate in Fig. 7 the large scale vertical motion at 15:00 UTC which is at the time the cirrus has already formed and is advecting toward the CF at SGP. The vertical velocity at 8–9 km height is approximately 0.01 m s^{-1} .

3.4.2 RUC model results

The regional (large-scale for our 10km domain high resolution simulations) scale up-draft is obtained using the profiles from the objective analysis with the Rapid Update Cycle (RUC) operational atmospheric prediction system. RUC is an analysis system and numerical forecast model which had its origins in the Mesoscale Analyses and Prediction System (MAPS) which was developed at the Forecast Systems Laboratory (FSL) in 1988. The first RUC model with a 3 h data assimilation cycle, 60 km resolution, and vertical 25 levels was established at the National Center for Environmental prediction (NCEP) in 1994. In 1998, this was followed by the RUC-2 model which had a 1 h data assimilation cycle, 40 km resolution and 40 levels. RUC-20 (20 km resolution, 50 levels) and RUC13 (13 km resolution, 50 levels) were developed in 2002 and 2005 separately. Providing short range weather forecasts is the primary use of RUC model and evaluation of other models. The diagnostic variables derived from RUC model is list in Table 2.

The RUC model being initialised with updated data every hour is a great strength as well as the fact that all the data are on isentropic vertical levels. The horizontal resolution, however, is a weakness for this case as it is still insufficient to describe local topographical circulations for this high resolution case.

For 9 March, the RUC model indicates little to no ascent rate (approximately zero and certainly bounded by 0.1 m s^{-1}) in the region in which the cirrus cloud is formed. So in summary, the objective analysis indicates a weak ascent whereas the RUC model indicates essentially no ascent. Since the objective analysis is making use of observed data local to where the cloud is observed and this data may contain signatures in the data of local forcings, we seek to explain the difference in forcings between the objective analysis results and the RUC model prediction.

Given that direction of the mean atmospheric flow at cloud level is over the Rocky Mountains on 9 March and the SGP CF is on the lee side of the mountains, the vertical motion could be explained by gravity waves. This could explain why the objective

[Title Page](#)

[Abstract](#)

[Introduction](#)

[Conclusions](#)

[References](#)

[Tables](#)

[Figures](#)

[⏪](#)

[⏩](#)

[◀](#)

[▶](#)

[Back](#)

[Close](#)

[Full Screen / Esc](#)

[Printer-friendly Version](#)

[Interactive Discussion](#)



analysis suggested a larger vertical velocity than the RUC model. In order to evaluate the potential of gravity waves to influence the cirrus formation, we have performed gravity wave simulations for the whole of the USA for 9 March 2000 using the model 3DVOM described in the next section.

3.4.3 Gravity wave analysis using 3DVOM

As shown in Fig. 8, the most prominent topological feature in this map of the USA is the Rocky Mountains (RM). The RM extend for more than 3000 miles in length and cover approximately 300 000 square miles and are positioned to the west of the SGP ARM site. With a south-west atmospheric advection, the influence of gravity waves on the cirrus formation on the lee side of the mountains is highly likely.

In this study, we make use of the 3DVOM model called 3-D velocities over mountains which is a finite-difference numerical model designed for high-resolution simulations of lee waves generated by flow over complex terrain.

The model is based on a set of time-dependent, simplified, quasi-linear equations of motion for a dry atmosphere (see Vosper and Worthington 2002, 2003 for details), typically run with European Centre for Medium Range Weather Forecasting (ECMWF) winds. The model was run at 1 km resolution for the entire USA, initialised in this case with NCEP winds and the topology specified from the data that went into making Fig. 8.

The resulting map of gravity wave vertical motion determined by 3DVOM at the cloud level is shown in Fig. 9. It shows clearly that gravity waves are predicted to cause ascending motion in the region where the cloud forms (roughly 300 km upwind) and during much of its advection toward the SGP CF site. Consequently, to obtain the vertical forcing for the high resolution cloud resolving simulation, we extracted the vertical forcing from Fig. 9 along the advection path of the cirrus cloud from formation to the SGP CF. The gravity wave forcing at cirrus cloud level as a function of time is given in Fig. 10.

The plot of vertical velocity forcing as a function of time, shown in Fig. 10, indicates gravity waves superimposed with various wavelengths that are undergoing an ascent

Title Page

Abstract

Introduction

Conclusions

References

Tables

Figures

◀

▶

◀

▶

Back

Close

Full Screen / Esc

Printer-friendly Version

Interactive Discussion



GCSS WG2 – case study

H. Yang et al.

[Title Page](#)[Abstract](#)[Introduction](#)[Conclusions](#)[References](#)[Tables](#)[Figures](#)[I◀](#)[▶I](#)[◀](#)[▶](#)[Back](#)[Close](#)[Full Screen / Esc](#)[Printer-friendly Version](#)[Interactive Discussion](#)

(hence cooling) beginning at the location where the cirrus is observed to first form. This agrees very well with where the cloud forms from satellite observation and the gravity wave forcing intensifies as the cloud advects toward the SGP site, in agreement with the satellite observation of the cloud intensifying as it advects to the CF. In the final stages of when the cloud is advecting over the SGP site, the gravity wave undergoes descent. So the modelled gravity wave forcing provides ascent or cooling to the cloud layer that is consistent with maintaining a cirrus cloud layer as it advects toward the CF site. We also note that the mean vertical velocity from the gravity wave simulation agrees well with the vertical velocity from the objective analysis. We would expect that the objective analysis would have been influenced by gravity waves whereas the RUC model would not.

4 Model setup and first results

We now describe how the observations were used to set up the modeling study and first results are illustrated just for the UK Met Office large eddy simulation model (LEM).

4.1 Inter-comparison model setup

The model domain size was 10 km in the horizontal by 20 km in the vertical. The horizontal resolution was set to 100 m and a variable vertical resolution was used with 100 m resolution in the cloud layer from 5 km to 10 km, with lower resolution above and below this region. The resolution was selected based on the aircraft turbulence analysis presented which indicated this was an appropriate scale in which to separate resolved and unresolved motions. The model simulation time was four hours duration. Time zero is associated with 14:00 UTC when the cloud first forms. No cloud is initially specified in the model; however, given the very slight supersaturation with respect to ice and the gravity wave forcing, a cloud develops right away so as to agree with the observations.

GCSS WG2 – case study

H. Yang et al.

[Title Page](#)[Abstract](#)[Introduction](#)[Conclusions](#)[References](#)[Tables](#)[Figures](#)[◀](#)[▶](#)[◀](#)[▶](#)[Back](#)[Close](#)[Full Screen / Esc](#)[Printer-friendly Version](#)[Interactive Discussion](#)

At the first time step of the simulation, random perturbations in potential temperature of $\pm 10\%$ and water vapour mixing ratio of $\pm 5\%$ are imposed between 6 and 10.5 km to establish initial inhomogeneity in the cloud layer (see Marsham and Dobbie, 2005).

We impose two forcings on the simulations in the inter-comparison, first a large scale gravity wave forcing updated every 201 s during the simulation. The gravity wave forcing is applied throughout the whole vertical domain for simplicity. Second, a Solar and infrared radiative heating profile is applied and updated every 5 min.

Periodic boundary conditions are used at the horizontal limits of the domain and in the vertical no slip conditions are imposed at the surface and top of the model atmosphere. Heterogeneous and homogeneous nucleation modes are permitted in the runs. Horizontal winds are specified from the radiosonde vector-resolved winds into the direction of the advection.

The Millimeter Cloud Radar (MMCR) based at the SGP CF is the key remote sensing tool used to obtain the comparison fields for this inter-comparison and so its location at CF is the point at which the cirrus cloud is compared quantitatively with the remote sensing. The cloud; however, forms approximately 300 km upwind from the CF. Thus it is necessary to either spin the cloud up to the observations at the CF or apply forcings that form the cloud when it is first noted to appear and let the cloud naturally evolve under the forcings and compare to observations when the cloud would be predicted to have crossed the SGP CF.

In the inter-comparison it was sought to form the cloud in the model based purely on the forcings acting to create the cloud rather than spin up the model cloud to artificially “agree” with an observed cloud which has a long history of evolution and is continuously changing as it advects over the observing point at the SGP Central Facility.

So we must recreate the conditions when the cloud was observed to form. We have a few constraints. From the satellite observations, the cirrus cloud was observed to first form at 14:00 UTC and took about 210 min to advect to the CF, roughly 300 km distance. Also, we know the thermodynamic profiles observed at the CF after the cloud advects to the CF. This is after the profiles have undergone forcings during the prior 210 min

during the time when the cloud advects from formation location to the CF. Therefore to obtain the profiles local to where the cloud formed we apply the forcing in reverse to obtain the initial profiles. This ensures that when the profiles are forced during the 210 min advecting to the CF they will then agree with the observed profiles.

5 We know the cloud first forms with the initial upwind profiles. It was necessary to adjust the initial cloud layer relative humidity to have a slight super-saturation with respect to ice of 10 %. This was equivalent to applying a small temperature adjustment of 1–2 K in the cloud layer, which is within observed error, so as to ensure that cloud formation occurred immediately (as observed) when modelled. With this small adjustment, the
10 cloud forms at the observed time. The initial profiles are shown in Fig. 11. To ensure that the small adjustment did not dictate the cloud ice water content when compared to observations at 210 min, runs were performed without the gravity wave forcing applied (only the small initial super-saturation remained). The cloud initially formed a low ice water content cloud that dissipated quickly. Therefore the small adjustment ensured
15 that the cloud formed at the observed time and that the cloud ice water content of the simulation was dictated by the gravity wave forcings and not due to uncertainty in the initial profile.

The above modelling case ensures that the cloud forms at the correct time and evolves under the influence of external gravity wave forcing and can be compared to observations at the CF after the 210 min duration of model run. For the initial comparison we used a 2-D simulation and performed the run for a four hour duration and compared with observations at 210 min. The 2-D domain is not for the full 300 km domain which would be too computationally taxing for high resolution simulations, not to mention problematic for periodic boundary conditions and a spatially varying forcing. The horizontal domain is 10 km which is taken to be a local region of cloud. The domain should be viewed as a Lagrangian domain advecting (and so advective tendencies which are small are ignored) with the mean wind from the cloud formation site to the CF site. The initial profiles of wind have their shape maintained so as to ensure the correct shear is used in the simulation, which is essential. The cirrus layer is completely detached
25

GCSS WG2 – case study

H. Yang et al.

Title Page

Abstract

Introduction

Conclusions

References

Tables

Figures



Back

Close

Full Screen / Esc

Printer-friendly Version

Interactive Discussion



from surface and boundary layer influences and so the mean wind-field is not important. First results are shown for LEM 2-D simulations described in the next section. The case data files are available at: <http://homepages.see.leeds.ac.uk/~lecsjed/huiyi/gcss/>.

4.2 First model comparisons to the GCSS case study

5 The UK Met Office LEM model version 2.3 was used to do a first test simulation of the case to evaluate the performance of a representative high resolution cloud model in preparation for the inter-comparison. Figure 12 shows the results of the LEM simulation at four times: 60 120, 180, and 210 min. 210 min is when the cirrus cloud is to be compared to observations. The growth and then decay of the ice water mixing ratio (IWMR) in Fig. 12 illustrates the importance of the gravity wave forcing on dictating the time evolution of the cirrus cloud.

10 In Fig. 13, we compare the cirrus to the observations, comparing iwmr to the observations at 210 min. We see that the magnitude of the cloud iwmr is similar at just over $2 \times 10^{-7} \text{ kg kg}^{-1}$. No tuning of parameters was performed in the model run. We note that the cloud depth is approximately 800 to 900 m thick in both the observed and the modeled results. There is however a difference in the vertical height of cloud base and top of roughly 400 to 500 m. Given that we have to initialise with vertical profiles from the CF (modified by the gravity wave) and the gravity wave forcing in the model is applied as a cooling (or warming) with no actual layer lift or descent the results are reasonable. By ensuring in our initial profiles that the cloud forms at the observed time and is dictated by the gravity forcing, the difference to the vertical profile is acceptable. A more detailed comparison of the modeled cloud to the observations including ice number concentration and fall speed is contained in the follow-on GCSS inter-comparison paper. We now present radiative heating rates and then finish with discussing two important sensitivities in the case.

25 The radiative heating profile for both solar and infrared (IR) was also output by the LEM model and applied in the inter-comparison. The radiative heating by Solar and IR at the times of 60, 120, 180, and 210 min are shown in Fig. 14. The radiative forcing

Title Page

Abstract

Introduction

Conclusions

References

Tables

Figures

◀

▶

◀

▶

Back

Close

Full Screen / Esc

Printer-friendly Version

Interactive Discussion



profiles were prepared for the inter-comparison at intervals of 5 min, which is deemed acceptable by assessing the rate of changes in cloud ice water content.

We now discuss a couple of key sensitivities for the case. Sensitivities of the runs to heterogeneous and homogeneous nucleation were investigated since the cloud temperature was about -38°C , and hence it was possible for heterogeneous and homogeneous nucleation to play a role. We allowed both nucleation modes to be on in the inter-comparison runs; however, since the ascent rate is weak heterogeneous nucleation was the dominant mode in the cloud formation. Runs with only homogeneous nucleation switched on required much greater initial super-saturation (or much stronger forcings), which did not agree with the water vapour profile at the time of cloud formation.

The models involved in the GCSS inter-comparison range from 1-D through to 3-D and so it was important to assess the influence that model dimensionality has on the case. To-date, there does not exist in the literature a testing of sensitivity of cirrus to model dimensionality for a wide range of forcings or specifically for the magnitude of forcing that is applied in this case. To illustrate the importance of dimensionality on our case, we present model results in Fig. 15 showing the combinations of ratios of 1-D and 2-D to 3-D results. The clouds are setup in the same manner as the standard case developed in this study except for the 1-D runs, where we used an ensemble of 30 1-D runs since the 1-D results are initialised with a single random perturbation in each vertical level. So different random perturbations were used for each run in the ensemble. The ensemble average of IWP was compared to 3-D model results.

It is shown in Fig. 15 that the 1-D to 3-D differ by as much as a factor of two (for appreciable ice water paths) early on in the simulation; however, at the comparison time of 210 min the difference is reduced significantly. The 2-D run compares well with the 3-D run for the full duration of the simulation so it illustrates that it is appropriate to use 2-D simulations for this case without significant differences to 3-D simulations for IWMR.

[Title Page](#)

[Abstract](#)

[Introduction](#)

[Conclusions](#)

[References](#)

[Tables](#)

[Figures](#)

[I◀](#)

[▶I](#)

[◀](#)

[▶](#)

[Back](#)

[Close](#)

[Full Screen / Esc](#)

[Printer-friendly Version](#)

[Interactive Discussion](#)



5 Conclusions

The main aim of the current GCSS cirrus inter-comparison was to evaluate models using observations. The last cirrus inter-comparison showed a huge range of results for ice water content with time for different models; however, the case was idealized and so observations were not available to distinguish between the performance of individual models or the modelling as a whole. The range of results shown in the last inter-comparison illustrated significant differences that at times were up to two orders of magnitude for ice water path between models as a function of time. This range of model results for a simplified case has raised concerns about the accuracy of cirrus modeling and so we need continued, detailed comparison cases to well observed cases. The case described in this work is an important step toward achieving that goal.

The 9 March 2000 cirrus case observed as part of the ARM SGP IOP during the month of March was selected primarily because the cloud was one of the best observed cases of cirrus with the cloud remote sensing and aircraft observations already analysed. The case has valuable remote sensing utilizing the radar, radiometers, and radiosonde measurements to derive the ice water content, ice number concentration, and fall speed of ice particles. The benefit of having all three to test models with is that it tests the models in far more rigorous ways than a single comparison against, for example, just ice water content.

The case has been formed utilizing GOES satellite observations to determine the approximate time of cloud formation, and the cloud forcing which is critical to the cloud development and evolution has been assessed using the RUC model, objective analysis as well as an application of the 3DVOM gravity wave model applied to the whole USA to determine the gravity wave forcing acting on the cloud layer. We find that the objective analysis and gravity wave simulations agree and that the gravity wave simulations correctly predict the time of the onset of the cloud.

Initial modelling results were obtained using the UK Met Office LEM in 2-D mode. The resolution of the model runs was established by analysis of the aircraft turbulence

GMDD

4, 2751–2790, 2011

GCSS WG2 – case study

H. Yang et al.

[Title Page](#)

[Abstract](#)

[Introduction](#)

[Conclusions](#)

[References](#)

[Tables](#)

[Figures](#)



[Back](#)

[Close](#)

[Full Screen / Esc](#)

[Printer-friendly Version](#)

[Interactive Discussion](#)



GCSS WG2 – case study

H. Yang et al.

[Title Page](#)[Abstract](#)[Introduction](#)[Conclusions](#)[References](#)[Tables](#)[Figures](#)[I◀](#)[▶I](#)[◀](#)[▶](#)[Back](#)[Close](#)[Full Screen / Esc](#)[Printer-friendly Version](#)[Interactive Discussion](#)

observations, which indicated that the inertial subrange was at approximately 100 m. The model runs were developed as a Lagrangian 10 km domain moving with the mean advective velocity of the cloud layer. Results from these simulations indicate that the cloud ice water content and cloud thickness are in good agreement. Difference is noted in the cloud base and top locations and attributed to having to initialise with profiles that were derived from observations at the SGP CF. The cirrus cloud forms at the correct time, within observational error, under the forcing of gravity waves that were derived from the advection trajectory through the results of the 3DVOM gravity wave simulations.

Some important sensitivities were tested such as the dominant nucleation mode which was determined to be heterogeneous nucleation. This was due to the weak forcing observed for the case. In addition, the model dimensionality was tested given that the inter-comparison will involved models running in 1-D, 2-D, and 3-D. It was found that the 2-D performed similar to 3-D for the whole run whereas the 1-D model agreed towards the end of the run but showed a factor of two difference in ice water mixing ratio early on in the cloud evolution.

This paper presents the current GCSS cirrus inter-comparison case which has been run by models ranging from highly detailed cirrus models through to GCMs with inter-comparison results presented in a follow-on paper. The intention this work was to provide a well characterised case study that can be used not only for the inter-comparison but will remain available to cirrus modelers for the future so that model updates and development of new cirrus models can be tested within its framework. We evaluate in the inter-comparison follow-on work if cirrus models have improved over the last decade. Although one detailed comparison case is not enough to comprehensively test a cirrus model in all scenarios, this well characterised case is an important step forward to evaluating our current capability in cirrus modelling.

Acknowledgements. Thanks for the Atmospheric Radiation Measurement (ARM) program for providing data. We acknowledge Jon Petch (UK Met Office) as first mentioning potential gravity wave influences for the case. Thanks for the UK Met Office for PhD part-funding for Huiyi Yang.

References

- Benedetti, A. and Stephens, G. L.: Characterization of errors in cirrus simulations from a cloud resolving model for application in ice water content retrievals, *Atmos. Res.*, 59-60, 393–417, 2001. 2754
- 5 Brown, P. R. A. and Heymsfield, A. J.: The microphysical properties of tropical convective anvil clouds: A comparison of models and observations, *Quart. J. Roy. Meteor. Soc.*, 127, 1535–1550, 2001. 2754
- Cheng, W. Y. Y., Wu, T., and Cotton, W. R.: Large-eddy simulation of the 26 november 1991 fire ii cirrus case. *J. Atmos. Sci.*, 58, 1017–1034, 2001. 2754
- 10 Cressman, G. P.: an operational objective analysis scheme, *Mon. Weather Rev.*, 87, 367–374, 1959. 2760
- Delanoe, J. and Hogan, R. J.: A variational scheme for retrieving ice cloud properties from combined radar, lidar and infrared radiometer, *J. Geophys. Res.*, 113, D07204, doi:10.1029/2007JD009000, 2008. 2754
- 15 Deng, M. and Mace, G. G.: Cirrus microphysical properties and air motion statistics using cloud radar doppler moments, part i: Algorithm description, *J. Appl. Meteor. Climatol.*, 45, 1690–1709, 2006. 2754
- Dobbie, S. and Jonas, P.: Radiative influences on the structure and lifetime of cirrus clouds, *Quart. J. Roy. Meteor. Soc.*, 127, 1–20, 2001. 2755, 2756
- 20 Dobbie, J. S., Li, J. N., and Chylek, P.: Two- and four-stream optical properties for water clouds and solarwavelengths, *J. Geophys. Res.*, 104, 2067–2079, 1999.
- Dowling, D. R. and Radke, L. F.: A summary of the physical properties of cirrus clouds, *J. Appl. Meteorol.*, 29, 970–978, 1990. 2758
- Fu, Q.: An accurate parameterization of the solar radiative properties of cirrus clouds for climate models, *J. Climate*, 9, 2058–2082, 1996. 2756
- 25 Fu, Q. and Liou, K. N.: Parameterization of the radiative properties of cirrus clouds, *J. Atmos. Sci.*, 50, 2008–2025, 1992.
- Fu, Q. and Liou, K. N.: On the correlated k-distribution method for radiative transfer in non-homogeneous atmospheres, *J. Atmos. Sci.*, 49, 2139–2156, 1993.
- 30 Fu, Q., Yang, P., and Sun, W. B.: An accurate parameterization of the infrared radiative properties of cirrus clouds for climate models, *J. Climate*, 11, 2223–2237, 1998. 2756
- Gray, M. E. B., Petch, J., Derbyshire, S. H., Brown A. R., Lock, A. P., Swann, H. A., and Brown,

[Title Page](#)

[Abstract](#)

[Introduction](#)

[Conclusions](#)

[References](#)

[Tables](#)

[Figures](#)

[I◀](#)

[▶I](#)

[◀](#)

[▶](#)

[Back](#)

[Close](#)

[Full Screen / Esc](#)

[Printer-friendly Version](#)

[Interactive Discussion](#)



GCSS WG2 – case study

H. Yang et al.

[Title Page](#)[Abstract](#)[Introduction](#)[Conclusions](#)[References](#)[Tables](#)[Figures](#)[⏪](#)[⏩](#)[◀](#)[▶](#)[Back](#)[Close](#)[Full Screen / Esc](#)[Printer-friendly Version](#)[Interactive Discussion](#)

P. R. A.: Version 2.3 of the met office large eddy model, Part ii: Scientific documentation, 2001. 2755

Li, J. and Dobbie, J. S.: Four-stream isosector approximation for solar radiative transfer, *J. Atmos. Sci.*, 55, 558–567, 1997. 2756

5 Lin, R. F., Starr, D. O., Demott, P. J., Cotton, R., Sassen, K., Jensen, E., Karcher, B., and Liu X. H.: Cirrus parcel model comparison project. phase 1: The critical components to simulate cirrus initiation explicitly. *J. Atmos. Sci.*, 59, 2035–2329, 2002. 2753, 2754

Liou, K. N.: Influence of cirrus clouds on weather and climate processes: a global perspective, *Mon. Weather Rev.*, 114, 1167–1199, 1986. 2756

10 Mace, G. G.: Cirrus layer microphysical properties derived from surfacebased millimeter radar and infrared interferometer data, *J. Geophys. Res.*, 103, 23207–23216, 1998. 2755, 2758

Marsham, J. and Dobbie, S.: The effects of wind shear on cirrus: A largeeddy model and radar case-study, *Quart. J. Roy. Meteor. Soc.*, 131, 2937–2955, 2005. 2754, 2755, 2756, 2765

15 Marsham, J., Dobbie, S., and Hogan, R.: Evaluation of a large-eddy model simulation of a mixed-phase altocumulus cloud using microwave radiometer, lidar and doppler radar data, *Quart. J. Roy. Meteor. Soc.*, 132, 1693–1715, 2006. 2754, 2755, 2756

Mason, P.: Large eddy simulation of the convective boundary layer, *J. Atmos. Sci.*, 46, 1492–1516, 1989.

20 Matrosov, S. Y., Uttal, T., Snider, J. B., and Kropfli, R. A.: Estimation of ice cloud parameters from ground-based infrared radiometer and radar measurements, *J. Geophys. Res.*, 97, 11567–11574, 1992. 2758

Matrosov, S. Y., Orr, B. W., Kropfli, R. A., and Snider, J. B.: Retrieval of vertical profiles of cirrus cloud microphysical parameters from doppler radar and infrared radiometer measurements, *J. Appl. Meteorol.*, 33, 617–626, 1994. 2758

25 Phillips V. T. J. and Donner L. J.: Cloud microphysics, radiation and vertical velocities in two- and three-dimensional simulations of deep convection, *Quart. J. Roy. Meteor. Soc.*, 132, 3011–3033, 2007.

Randall, D., Curry, J., Duynkerke, P., Miller, M., Moncrieff, M., Ryan, B., Starr, D., and Rossow, W.: The second gewex cloud system study science and implementation plan, IGPO Publication Series, 34, 2000. 2753

30 Solch, I. and Kaercher, B.: Process-oriented large-eddy simulations of a midlatitude cirrus cloud system based on observations, *Quart. J. Roy. Meteor. Soc.*, 137, 374–393, 2001. 2754

Starr, D.-C., Benedetti, A., Boehm, M., Brown, P. R. A., Gierens, K. M., Girard, E., Giraud, V.,

GCSS WG2 – case study

 H. Yang et al.

[Title Page](#)
[Abstract](#)
[Introduction](#)
[Conclusions](#)
[References](#)
[Tables](#)
[Figures](#)
[I◀](#)
[▶I](#)
[◀](#)
[▶](#)
[Back](#)
[Close](#)
[Full Screen / Esc](#)
[Printer-friendly Version](#)
[Interactive Discussion](#)


Jakob, C., Jensen, E., Khvorostyanov, V. I., Koehler, M., Lare, A., Lin, R.-F., Maruyama, K., Montero, M., Tao, W.-K., Wang, Y., and Wilson, D.: Comparison of cirrus cloud models: a project of the GEWEX Cloud System Study (GCSS) working group on cirrus cloud system, Proceedings of the 13th International Conference on Cloud and Precipitation (ICCP), Reno, NV, USA, 14–18 August 2000. 2753

Vosper, S. B.: Development and testing of a high resolution mountainwave forecasting system, *Met. Apps.*, 10, 75–86, 2003. 2763

Vosper, S. B. and Worthington, R. M.: Vhf radar measurements and model simulations of mountain waves wver wales, *Quart. J. Roy. Met. Soc.*, 128, 185–204, 2002. 2763

Yang, H., Dobbie, S., Herbert, R., Connolly, P., Gallagher, M., Ghosh, S., Al-Jumur, S. M. R. K., and Clayton, J.: The effect of observed vertical structure, habits, and size distributions on the Solar radiative properties and cloud evolution of cirrus clouds, submitted, 2011. 2754, 2755, 2756

Zhang, M. H. and Lin, J. L.: Constrained variational analysis of sounding data based on column-integrated budgets of mass, heat, moisture, and momentum: Approach and application to arm measurements, *J. Atmos. Sci.*, 54, 1503–1524, 1997. 2760, 2761

Zhang, M. H., Lin, J. L., Cederwall, R. T., Yio, J. J., and Xie, S. C.: Objective analysis of arm iop data: Method and sensitivity, *Mon. Weather Rev.*, 129, 295–311, 2000. 2757, 2760

GCSS WG2 – case study

H. Yang et al.

[Title Page](#)[Abstract](#)[Introduction](#)[Conclusions](#)[References](#)[Tables](#)[Figures](#)[I◀](#)[▶I](#)[◀](#)[▶](#)[Back](#)[Close](#)[Full Screen / Esc](#)[Printer-friendly Version](#)[Interactive Discussion](#)**Table 1.** The surface measurement used by the objective analysis at the ARM SGP site at Oklahoma USA, used for the objective analysis during the 9 March 2000 campaign and the variables measured by each instrument.

Platform Name	Variables Measured
Surface Meteorological Observation Stations (SMOS)	surface pressure, surface winds, temperature, humidity
Energy Budget Bowen Ratio (EBBR) Stations	surface latent and sensible heat fluxes, surface broadband net radiative flux
Eddy Correlation Flux Measurement System (ECOR)	surface vertical fluxes of momentum, sensible heat flux, latent heat flux
Oklahoma and Kansas mesonet stations (OKM and KAM)	surface precipitation, pressure, winds, temperature
Microwave Radiometer (MWR) stations	column precipitable water, total cloud liquid water
GOES satellite	clouds and broadband radiative fluxes

GCSS WG2 – case study

H. Yang et al.

Table 2. The diagnosed variables output by the Rapid Update Cycle (RUC) model.

Relative Humidity	Surface Temperature
Dew Point	Sea-level pressure
Precipitation	Snow accumulation
snow depth	Precipitation type
Freezing levels	3 h pressure changes
CAPE/CIN	Lifted Index
Precipitable water	Helicity
Soil moisture	Tropopause pressure
Vertical velocity	PBL depth
Gust wind speed	Cloud base height
Cloud fraction	Visibility
Pressure of max Theta-E in column	convective cloud top height
Equilibrium level height	

[Title Page](#)[Abstract](#)[Introduction](#)[Conclusions](#)[References](#)[Tables](#)[Figures](#)[I◀](#)[▶I](#)[◀](#)[▶](#)[Back](#)[Close](#)[Full Screen / Esc](#)[Printer-friendly Version](#)[Interactive Discussion](#)

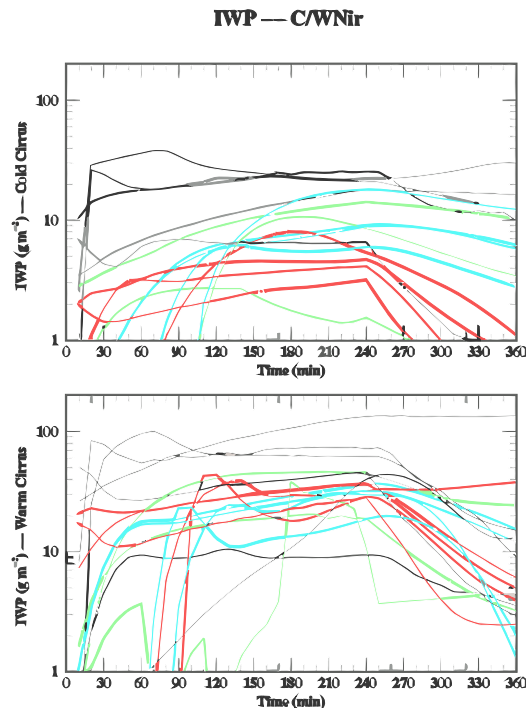


Fig. 1. Time series of vertically-integrated ice water path (g m^{-2}) from cirrus models, which participate the ICMCP. These baseline simulations correspond to night-time (infrared radiation only). The upper panel is for the “cold” (about -66°C) cirrus case and the bottom one is for the “warm” (about -47°C) cirrus case. A 3 cm s^{-1} uplift is continuously apply over a 4 h time, and then there is 2-h dissipation time. Color cyan represents CSMs with bin microphysics, red represents CSMs with bulk microphysics, green represents single column models and the thin black represents CSMs with heritage in study of deep convection or boundary layer clouds. This figure illustrates the wide range in cirrus model predictions for an idealised case (figure is taken from Starr et al., 2000).

[Title Page](#)[Abstract](#)[Introduction](#)[Conclusions](#)[References](#)[Tables](#)[Figures](#)[◀](#)[▶](#)[◀](#)[▶](#)[Back](#)[Close](#)[Full Screen / Esc](#)[Printer-friendly Version](#)[Interactive Discussion](#)

GCSS WG2 – case study

H. Yang et al.

Title Page

Abstract

Introduction

Conclusions

References

Tables

Figures

◀

▶

◀

▶

Back

Close

Full Screen / Esc

Printer-friendly Version

Interactive Discussion



Sonde data for 9 Mar 2000, 17:30:00
Skew-T, Log(P) Diagram

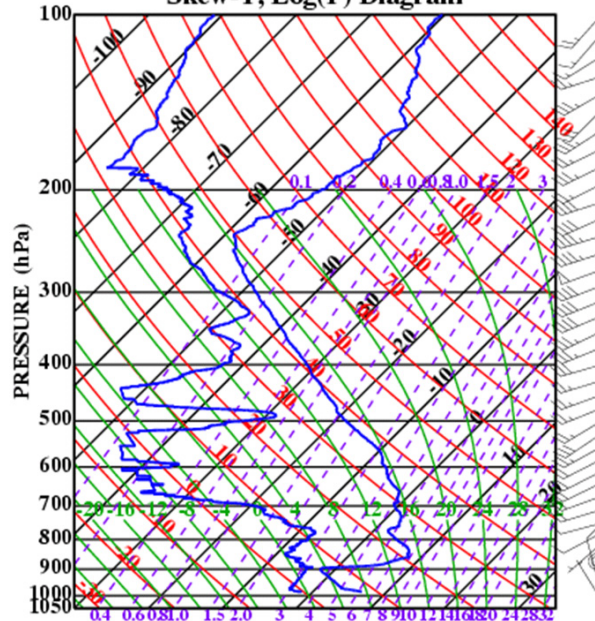


Fig. 2. Teph-graph for the 9 March 2000 case study. The meteorological soundings are taken from radiosonde ascents and indicate the high water vapour around the 500 mb level where the cloud forms.

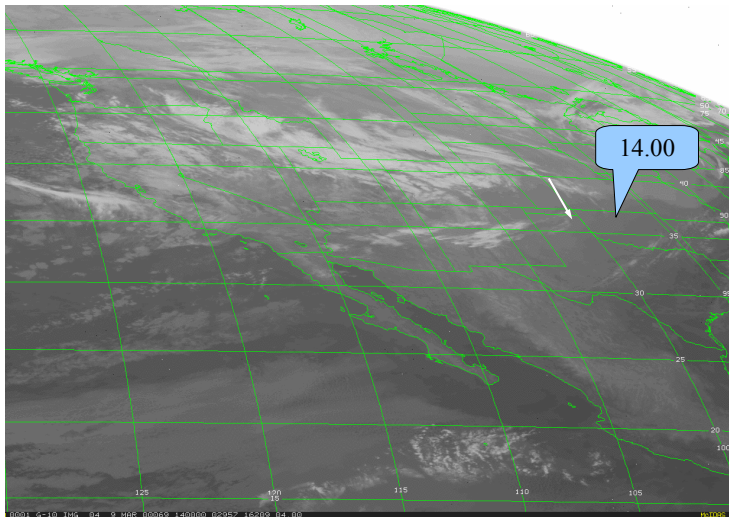


Fig. 3. GOES10 satellite plot at 14:00 on the 9 March 2000.

Title Page

Abstract

Introduction

Conclusions

References

Tables

Figures

⏪

⏩

◀

▶

Back

Close

Full Screen / Esc

Printer-friendly Version

Interactive Discussion



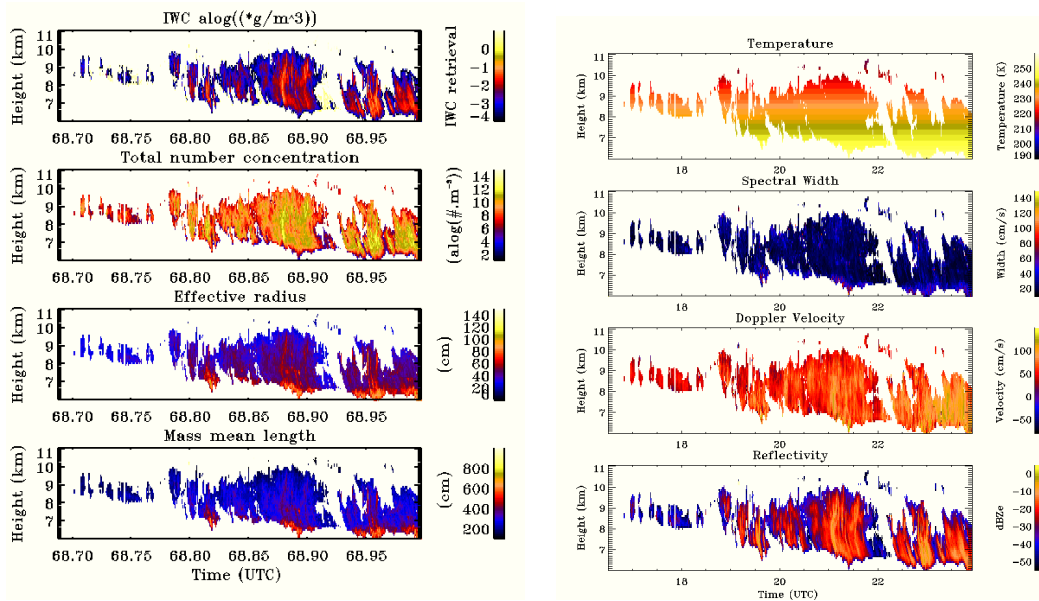


Fig. 4. Remotely sensed quantities as a function of height and time. The quantities include ice water content, total ice number concentration, effective radius, mean mass length, temperature, spectral width, Doppler velocity, and reflectivity. Units indicated in the plots. The plots based on retrievals at the ARM SGP Central Facility for 9 March 2000. The inter-comparison is based on the cloud when it first arrives at the Central Facility, as indicated on the left side of each plot.

[Title Page](#)
[Abstract](#)
[Introduction](#)
[Conclusions](#)
[References](#)
[Tables](#)
[Figures](#)
[◀](#)
[▶](#)
[◀](#)
[▶](#)
[Back](#)
[Close](#)
[Full Screen / Esc](#)
[Printer-friendly Version](#)
[Interactive Discussion](#)

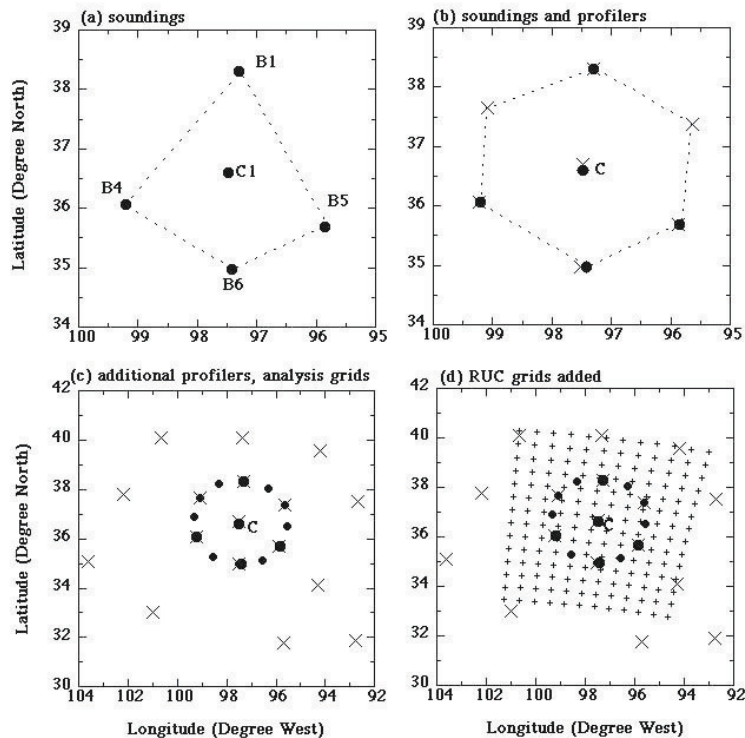



Fig. 6. Latitude and longitude locations of the (a) radiosonde launches, (b) the radiosonde launch sites and profiles, (c) additional profilers and grid, and (d) the RUC model grid. (The plots are taken from Zhang et al., 2000).

[Title Page](#)[Abstract](#)[Introduction](#)[Conclusions](#)[References](#)[Tables](#)[Figures](#)[I◀](#)[▶I](#)[◀](#)[▶](#)[Back](#)[Close](#)[Full Screen / Esc](#)[Printer-friendly Version](#)[Interactive Discussion](#)

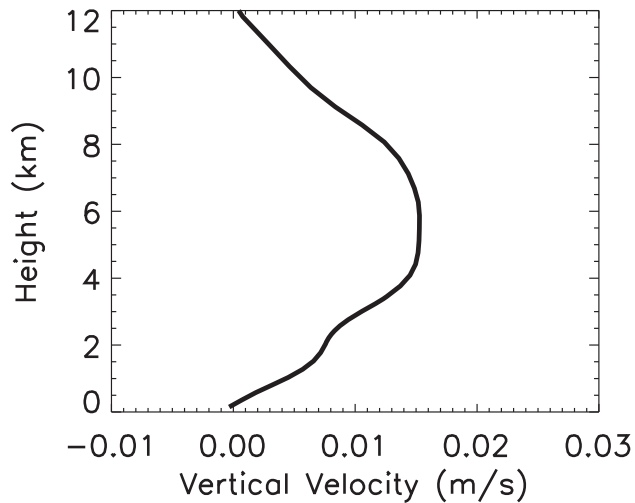


Fig. 7. Large scale vertical velocity from OA at 3 p.m., 9 March 2000.

GCSS WG2 – case study

H. Yang et al.

[Title Page](#)

[Abstract](#) [Introduction](#)

[Conclusions](#) [References](#)

[Tables](#) [Figures](#)

[◀](#) [▶](#)

[◀](#) [▶](#)

[Back](#) [Close](#)

[Full Screen / Esc](#)

[Printer-friendly Version](#)

[Interactive Discussion](#)



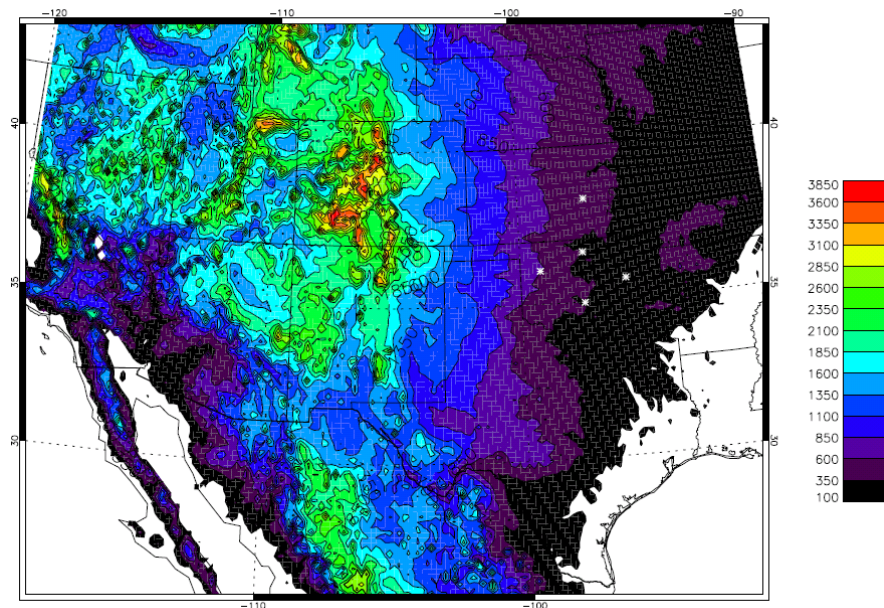


Fig. 8. Topology of the USA (m). This is used to initialise the surface heights for the gravity wave simulations in the 3DVOM model. The white dots indicate the ARM SGP Central and Boundary Facilities (Data provided by Andy Ross, University of Leeds).

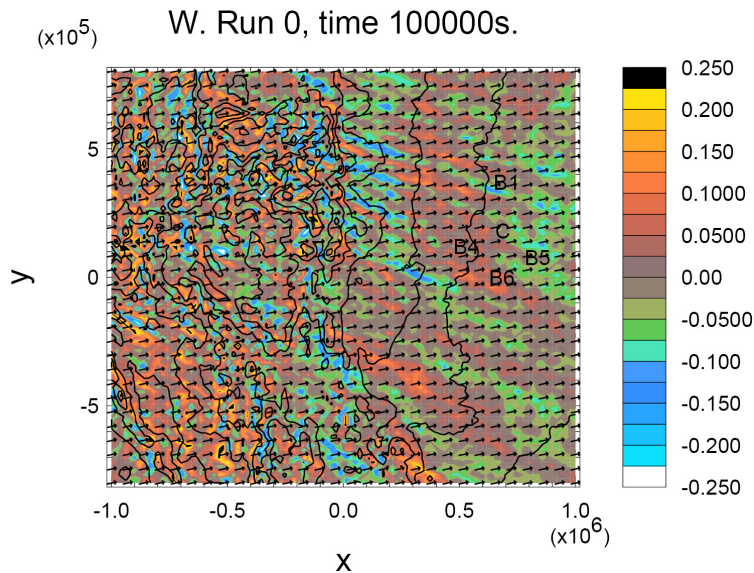


Fig. 9. Gravity wave plots at the cirrus level for 9 March 2000. Colour codes indicate ascent rate (positive) or descent (negative) in m s^{-1} . These results are derived from the output of 3DVOM model runs.

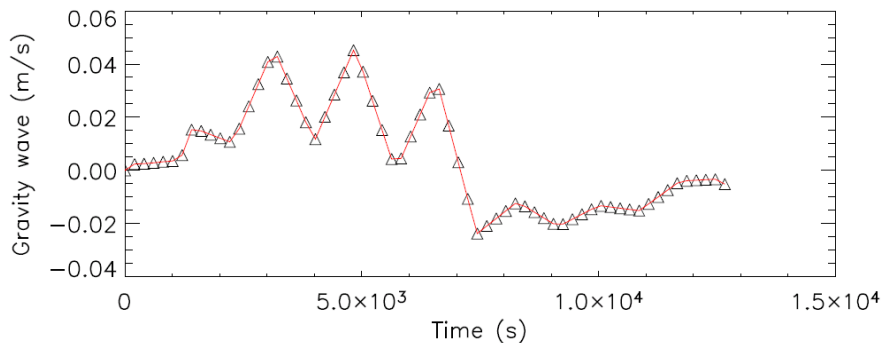


Fig. 10. Modelled gravity wave forcing (m s^{-1}) versus time (s). This is the modelled gravity wave forcing that the cloud experiences as it advects from where it first formed to when it arrives at the ARM SGP Central Facility, as observed by the MMCR radar.

Title Page	
Abstract	Introduction
Conclusions	References
Tables	Figures
◀	▶
◀	▶
Back	Close
Full Screen / Esc	
Printer-friendly Version	
Interactive Discussion	



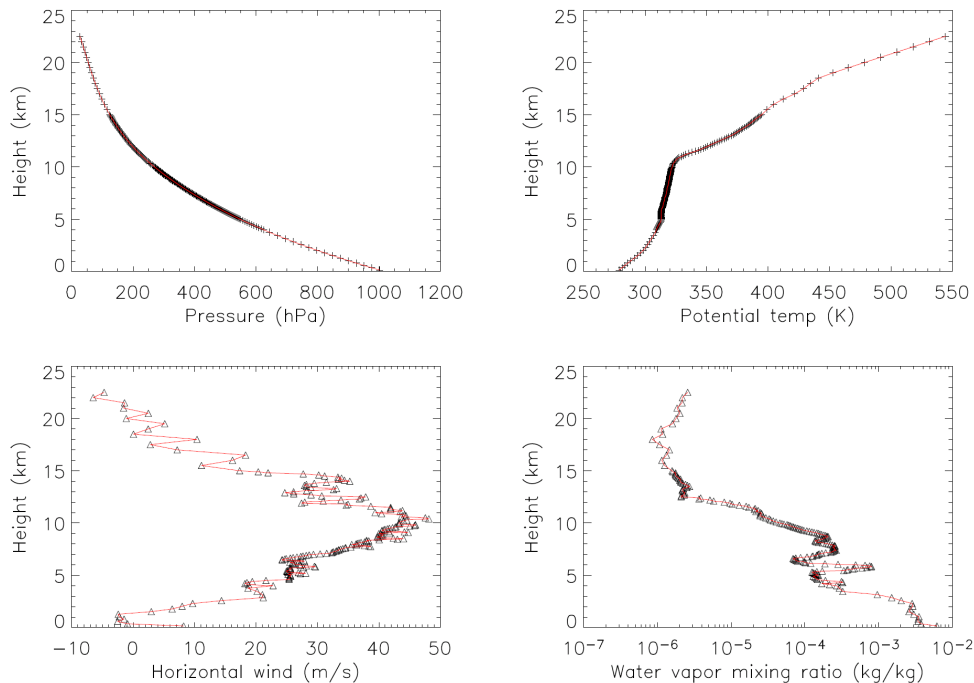
[Title Page](#)[Abstract](#)[Introduction](#)[Conclusions](#)[References](#)[Tables](#)[Figures](#)[◀](#)[▶](#)[◀](#)[▶](#)[Back](#)[Close](#)[Full Screen / Esc](#)[Printer-friendly Version](#)[Interactive Discussion](#)

Fig. 11. Initial profiles of pressure, potential temperature, horizontal wind, and water vapour mixing ratio at the start location upwind from the Central Facility. The profiles are obtained by taking the observed values at the Central Facility and backtracking them through the effects of the gravity wave to the starting location. This ensures that the profiles will be as observed after the effects of the gravity wave in the modelling.

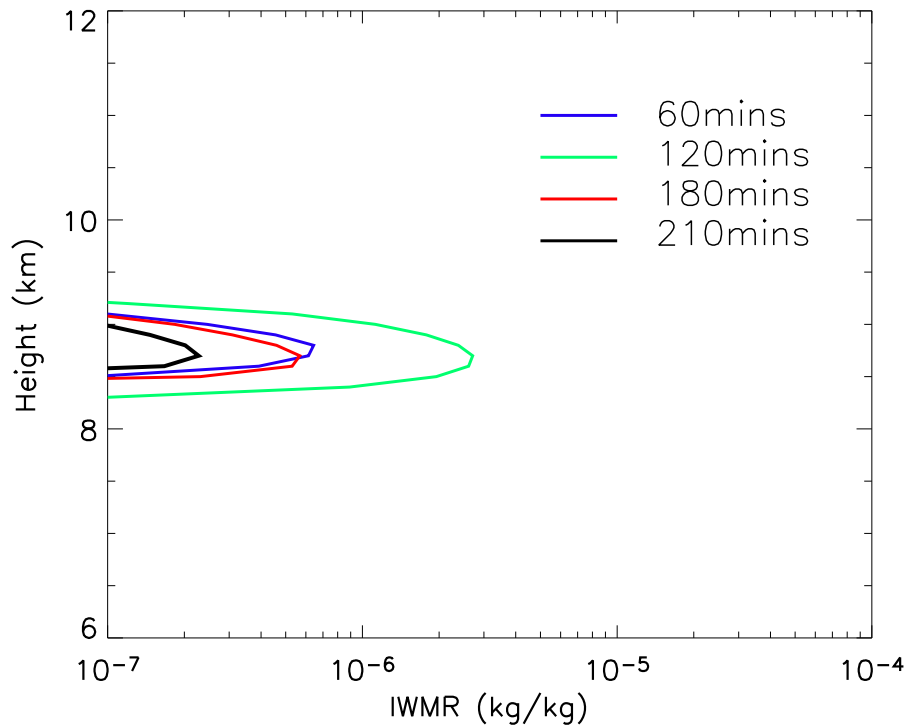


Fig. 12. Shown are the total ice water mass mixing ratio (kg kg^{-1}) (total indicates ice and snow which are ice aggregates in this simulation) versus height at four times during the UK Met Office LEM simulation: 60, 120, 180, and 210 min. The cirrus cloud modelled in the LEM is compared to observations at 210 min.

[Title Page](#)

[Abstract](#) [Introduction](#)

[Conclusions](#) [References](#)

[Tables](#) [Figures](#)

[◀](#) [▶](#)

[◀](#) [▶](#)

[Back](#) [Close](#)

[Full Screen / Esc](#)

[Printer-friendly Version](#)

[Interactive Discussion](#)



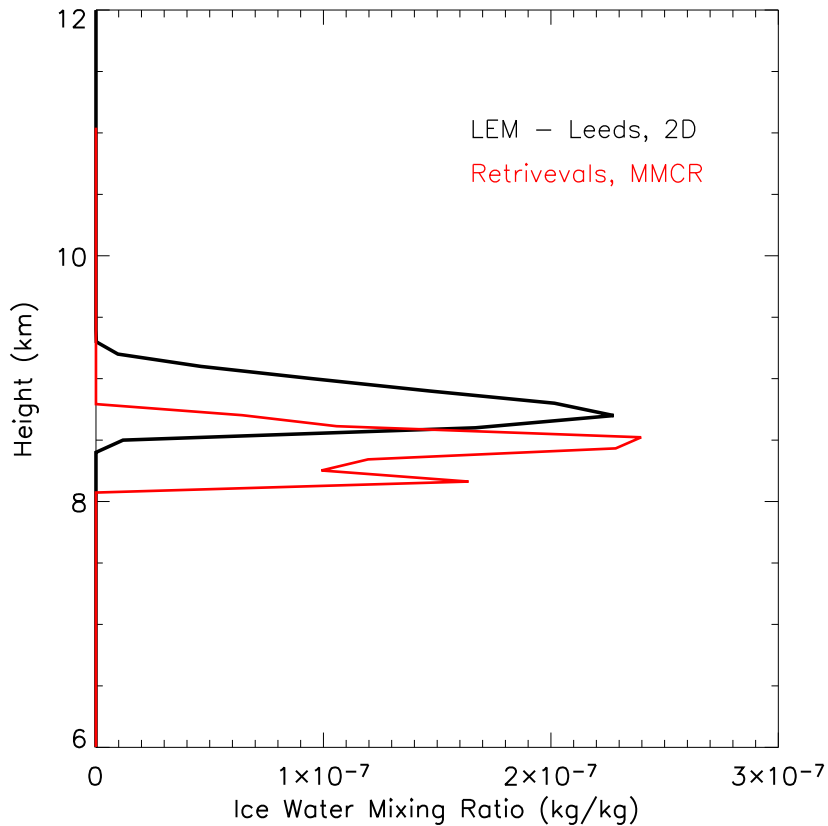


Fig. 13. Ice water mixing ratio (kg kg^{-1}) versus height (km). The retrieved values are indicated in red and the model simulation results are in black. The model output is taken from the UK Met Office LEM runs at 3.5 h after the start of the simulation, which is when the cloud passes over the Central Facility.

[Title Page](#)

[Abstract](#) [Introduction](#)

[Conclusions](#) [References](#)

[Tables](#) [Figures](#)

[◀](#) [▶](#)

[◀](#) [▶](#)

[Back](#) [Close](#)

[Full Screen / Esc](#)

[Printer-friendly Version](#)

[Interactive Discussion](#)



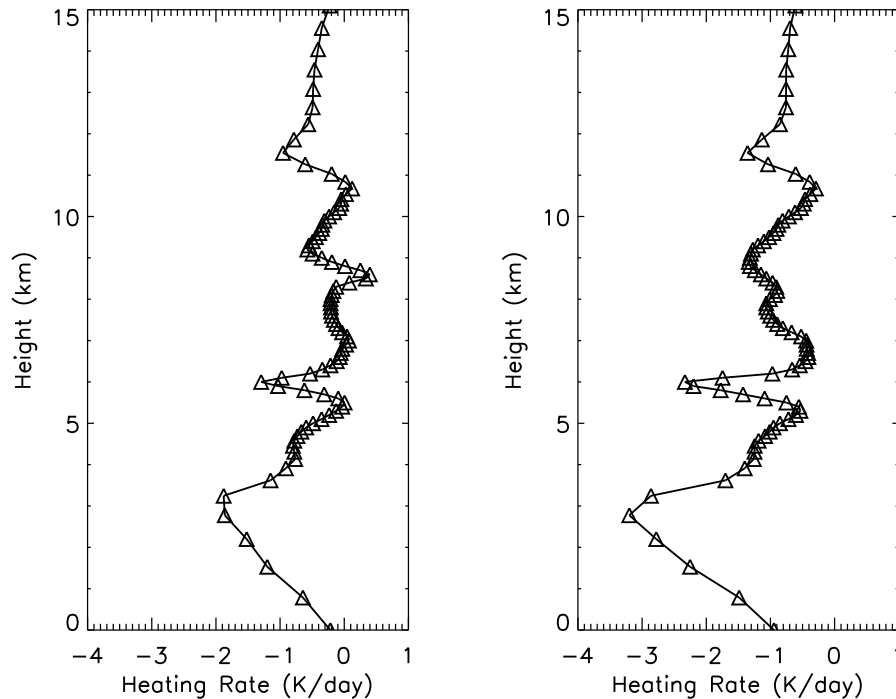


Fig. 14. Heating rate (K day^{-1}) profiles taken from the UK Met Office LEM model running with the Fu-Liou radiation scheme for 9 March 2000 at simulation times 120 and 210 min. The plots indicate very little variability in the heating rates except for about 8 to 9 km where the cloud forms and evolves.

Title Page	
Abstract	Introduction
Conclusions	References
Tables	Figures
◀	▶
◀	▶
Back	Close
Full Screen / Esc	
Printer-friendly Version	
Interactive Discussion	



GCSS WG2 – case study

H. Yang et al.

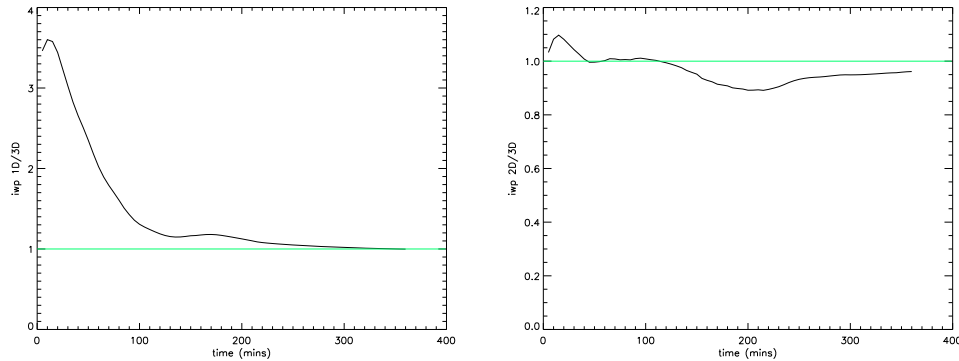


Fig. 15. Figure model dimensionality. Plot on the left is the division of 1-D and 3-D (1-D/3-D), and plot on right is the division of 2-D and 3-D (2-D/3-D).

[Title Page](#)[Abstract](#)[Introduction](#)[Conclusions](#)[References](#)[Tables](#)[Figures](#)[⏪](#)[⏩](#)[◀](#)[▶](#)[Back](#)[Close](#)[Full Screen / Esc](#)[Printer-friendly Version](#)[Interactive Discussion](#)